

Walther MAIER¹
Martin KIMMELMANN^{1*}

SPINDLE CRASH – BEARING DAMAGES DETECTED BY VIBRATION TESTS

This paper presents experiments regarding the collision of a main spindle with a fixed machine body, i.e. a machine crash. Using experimental tests, it is shown how a machine crash affects the main spindle and its components. After the crash test under laboratory conditions, damages in the form of constrictions and transverse grooves in the bearing rings of the hybrid bearings are detected with roundness tests. Focused on the effects of a crash on high-speed bearings, vibration analyses of the motor spindle are carried out before and after the spindle crash. This paper presents how experimental order tracking analysis and roundness tests can be used to draw conclusions about the spindles' state, especially about bearing damages caused by the collision.

1. INTRODUCTION

The service life of the main spindle's bearings in machine tools basically depends on the usage or rather the machining method, such as milling or grinding, as well as on the load arising during finishing, roughing, interrupted cutting or even chattering. However, damages to the spindle bearings can also be decisively caused by a possible collision of the spindle with the workpiece. An early failure of the main spindle then leads to high follow-up costs due to downtimes of the machine tool and a complete exchange for an analogous spindle.

A study by experts for breakdowns [5] showed that about 85 % of spindle failures result from bearing damages. According to this study, almost 50 % of these damages are due to wear, 10 % are due to dirt or insufficient lubrication and 40 % are due to machine collisions. According to other surveys, 35 % [1] or even 60 % [8] of failures regarding main spindles are caused by a spindle crash.

Hence, the Institute for Machine Tools of the University of Stuttgart conducted an experiment modelling a typical machine crash. In addition, by using so-called kinematic ball pass frequency analyses it was examined how a crash affects the dynamic behaviour of the spindle or the bearings after a collision. Hence, industry or rather the machine tool sector uses two systems to protect main spindles against bearing damages:

¹ University of Stuttgart, Institute for Machine Tools (IfW), Stuttgart, Germany

* E-mail: martin.kimmelman@ifw.uni-stuttgart.de

- collision protection systems for motor spindles or guideway systems,
- systems for machine diagnosis or for detecting bearing damages.

One of the best-known collision protection systems is offered by Hermle. Issued by the European Patent Office in 1999, the patent EP 0755750B1 [9] includes a collision protection with an aluminium compression sleeve and represents a unique selling proposition for the motor milling spindles by Hermle, which meets with great approval of the users. Other manufacturers and research institutions developed torque- or power-operated mechanical collision protection devices as well. Published in 2016, the dissertation by D. Korff [6] provides an extensive overview of these mechanical systems. Most of them, however, concern feed systems and/or have not been used in industry yet. Furthermore, there are a lot of condition monitoring systems using internal control signals, such as e. g. motor currents in the drives, to trigger a rapid switching off or an emergency stop, for example. Various conferences and papers are dedicated to condition monitoring so that it is not necessary to present these systems in this paper.

Numerous methods based on the spectral analysis of acceleration signals were developed for detecting damages of rolling bearings in machine tool spindles [3],[4]. These are basically aimed at detecting how damages to the raceway of rolling bearings spread, which are caused by the fatigue of the ring material due to the ball pass [2]. The approaches used here are basically based on detecting impulses caused by rolling across defects (pittings) in the raceway surface.

Damages to rolling bearings can arise here on the inner or outer ring, the rolling bearing itself or the rolling bearing cage. By kinematically modelling the rolling contact, it is possible to establish the ball pass frequencies of such defects for ideal rolling conditions, depending on the rotational frequency. By normalising the frequencies relative to the rotational speed, it is possible to directly calculate the order when passing over a defect instead of the frequencies. In this way a ball pass event can be directly related to the type of defect. The respective order of an excitation O_N can be inferred from the dimensions of the bearing with the parameters of rolling bearing like the diameter of the roller elements d , pitch circle diameter D_p and operating contact angle α as well as the number of rolling elements n_b . The excited orders due to a defect on the outer ring can be calculated with Equation (1), whereas those due to a defect on the inner ring can be calculated with Equation (2), cf. [7].

$$O_o = \frac{1}{2} O_N n_b \left(1 - \frac{d}{D_p} \cos(\alpha) \right) \quad (1)$$

$$O_i = \frac{1}{2} O_N n_b \left(1 + \frac{d}{D_p} \cos(\alpha) \right) \quad (2)$$

Apart from these orders excited by individual impulses, the sidebands can also be excited by a ball pass. These sidebands are excited by an amplitude modulation when the balls roll across a defect and are located in the frequency spectrum to the left and right of the excited order, each shifted by the modulation frequency. Consequently, the sidebands at a distance of one order or its multiples i can also be excited at $O_i \pm iO_N$ due to a defect in the rotating inner ring, cf. Equation (3) [10].

$$O_s = O_I \pm iO_N \quad (3)$$

In order to investigate the influence of a spindle crash on the bearing damages and the dynamic behaviour of a spindle system, this paper presents a methodical approach. The impact on the spindle to simulate a crash is performed on a test bench as shown in Chapter 2. After the crash, the damages on the raceway can be detected by measuring the roundness of the bearings' outer and inner rings as shown in Chapter 3. Before the crash, the vibrational characteristics of the spindle before a collision have to be tested to achieve a basis for comparing the behaviour before and after the collision as shown in Chapter 4. Therefore, it is recommended to perform run-up tests of the spindle to analyse the vibrational characteristics of the spindle. It can be shown that a spindle crash leads to a characteristic vibrational behaviour of the spindle, which can be deduced from specific stimulated orders of the system. A collision at rotational speed also leads to the specific formed grooves on the bearing raceway as shown in this paper.

2. COLLISION TEST STAND AND CRASH

A test stand for simulating machine crashes was developed, taking different designs into consideration and evaluating them. The intention was to develop a test set-up that can provide reproducible results without causing great damages to further machine elements. The crash or rather the impulse should be limited to one contact only. The acting force as well as the impulse energy should be variable. In the end the design of a drop hammer, similar to a guillotine, was realised. A dismantled machine frame with a base plate and a welded machine column was used as test stand. Linear rolling guideways were fastened to this vertical column. Therefore, the drop weight is led over the guideway system like a machine slide. The motor spindle is fastened to a horizontal plate on top of the test stand. A shop crane pulls the drop weight up to a given height and then drops it by means of a releasing mechanism. The rate of fall, the acting force and the contact times were examined in preliminary tests. Due to the kinematic design, the weight falls exactly and in a controlled way onto a test mandrel clamped into the spindle. A catching mechanism prevents the rebounding drop weight from hitting the test mandrel in the spindle several times.

In order to analyse the crash during the experiment, a measuring equipment was used consisting of a high-speed camera and a Dactron multi-channel data acquisition and analysis system with accelerometers for recording the accelerations. In the test presented here, the spindle rotated at a rotational speed of $n = 6,000 \text{ min}^{-1}$. The drop height was 0.41 m. A realistic impact of a drop weight falling onto a motor spindle at a speed of about 2.7 m/s and with a mass of about $m = 90 \text{ kg}$ was realised. Hence, the movement generates a kinetic energy of $E_{kin} = 328 \text{ J}$.

Figure 1 on the left depicts the CAD model of the test stand with a drop weight and a motor spindle in the crash position. The crashed spindle is a motor spindle by Hugo Reckerth GmbH, Stuttgart, Germany with a rated output of $P = 15 \text{ kW}$ at a maximum

rotational speed of $n_{max} = 24,000 \text{ min}^{-1}$. A solid tool mandrel was clamped into the motor spindle. Figure 1 on the right shows a photo of the test when the drop weight is in contact with the tool in the main spindle.

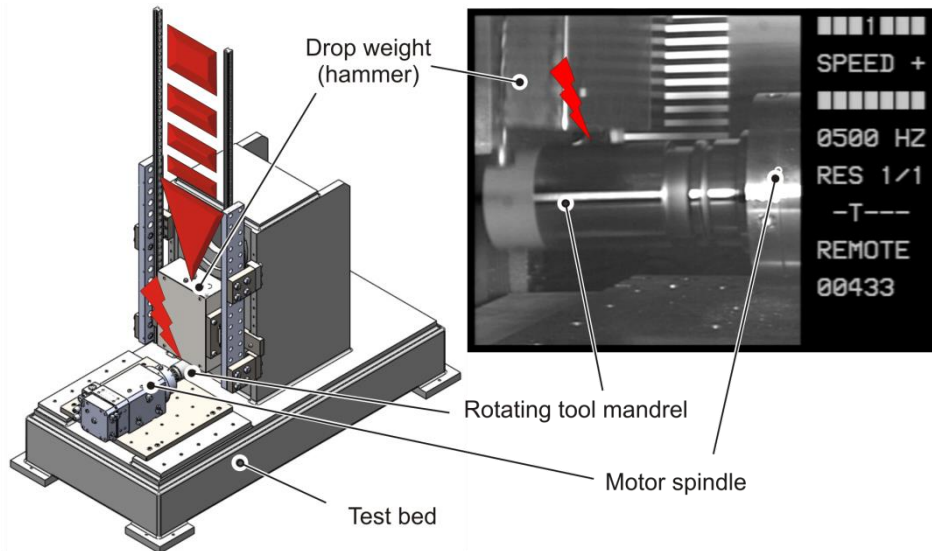


Fig. 1. CAD model of the test stand for simulating a spindle crash and a photo of the test, taken with a high-speed camera during the contact

The acceleration of the drop weight was recorded during the impact with a 500 g 3-axis accelerometer. In order to filter high-frequency vibrations out of the measuring signal, median and Savitzky-Golay filters were used for smoothing the acceleration curves. Using the acceleration data recorded, it is possible to establish the maximum acceleration of the drop weight as well as the time of impact. Figure 2 illustrates the filtered acceleration course of the drop weight.

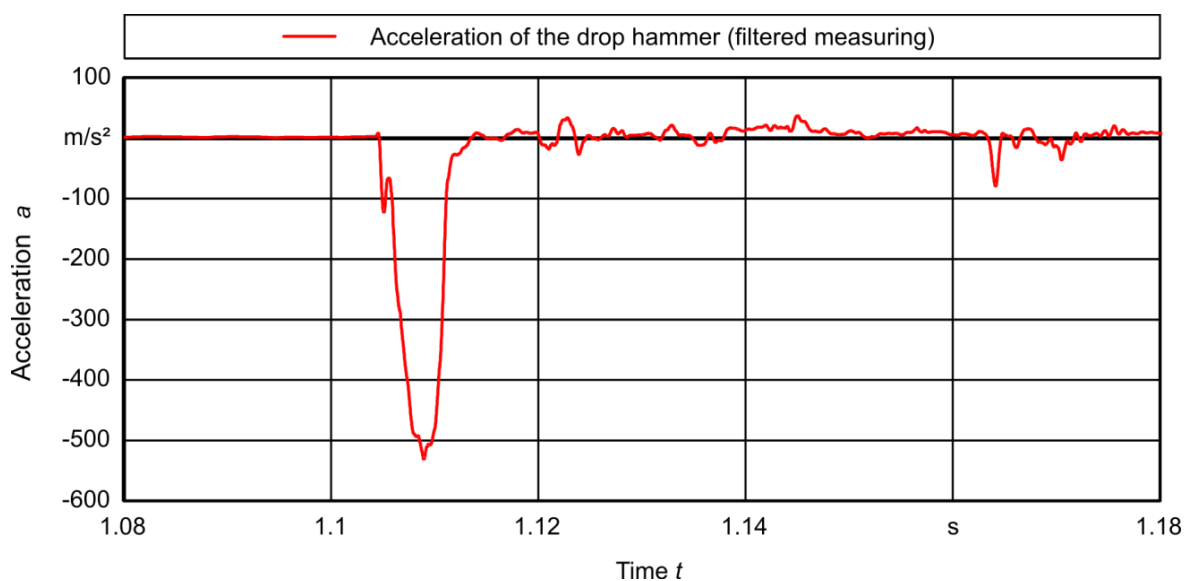


Fig. 2. Acceleration of the drop weight depending on time in the test with the rotating tool

The maximum acceleration on impact was approx. $a_{crash} = 530 \text{ m/s}^2$ in this test. Hence, a force of $F_{crash} = 48 \text{ kN}$ occurred as impact force. The contact time of the drop weight with the tool mandrel was approx. 7 ms. Analysing the photos taken with the high-speed camera produced roughly the same contact time (6 ms at approx. three photos and a measurement frequency of 500 Hz). Due to the loading the tool mandrel gave way, sprang back a little and finally broke after all.

In the crash test with the rotating spindle, the test mandrel suffered a brittle fracture upon impact. After breaking, it spun for approximately another 0.1 seconds. The motor spindle was running considerably longer until it came to a standstill. Due to the impact the collet chuck could not release the hollow shaft taper's remains of the test mandrel, so that these remains and the bearings had to be dismantled by the manufacturer. When the spindle was coming to a standstill, a rattling noise of the bearings could be heard already.

3. MEASURING THE GEOMETRY OF THE BEARING RINGS AFTER THE CRASH

The motor spindle contains a high-speed spindle bearing with hybrid bearings, type 7009 CE/HC by SKF, placed as set of bearings with three bearings at the front in tandem-O-arrangement and two bearings at the rear in tandem arrangement (cf. Table 1).

Table 1. Properties of the spindle bearings

| | |
|----------------------------|---------|
| type of bearing | hybrid |
| size | 7009 |
| outside diameter D [mm] | 75 |
| bore diameter d [mm] | 45 |
| number of balls n_b | 21 |
| ball diameter D_b [mm] | 7.14 |
| Ring width B [mm] | 16 |
| ball material | ceramic |
| contact angle α [°] | 15 |

The bearings were measured with a roundness measuring instrument by Taylor Hobson (Talyrond), and the results were evaluated with a Matlab program. A stylus with a 1 mm ball was used for the tactile measurement. When measuring the outer ring, it was possible to choose a vertical orientation of the stylus over nearly the complete inside. Regarding the inner ring, the stylus device had to be swivelled by an angle of over 10° in the raceway, leading to a minor measuring error.

The outer ring of the front bearing got a necking of max $13.2 \mu\text{m}$ due to the crash. This necking is greatest close to the thinnest area of the bearing ring. It can, however, be detected along the entire width of the bearing ring as well.

Figure 3 presents the measurement of the roundness in the raceway of the outer ring in the front bearing. The roundness was measured here at a height of 9.2 mm from the narrow side of the outer ring. Well visible are the necking, which leads to a roundness deviation

of $9.8 \mu\text{m}$, as well as three great and two small transverse grooves, caused by the ceramic balls due to plastic deformation. The three great grooves are about 17.1° apart from each other. The arithmetical distance between two balls is $360^\circ:21=17.14^\circ$ as well. The transverse grooves are up to about $1.5 \mu\text{m}$ deep and about 1.2° or rather 0.7 mm wide.

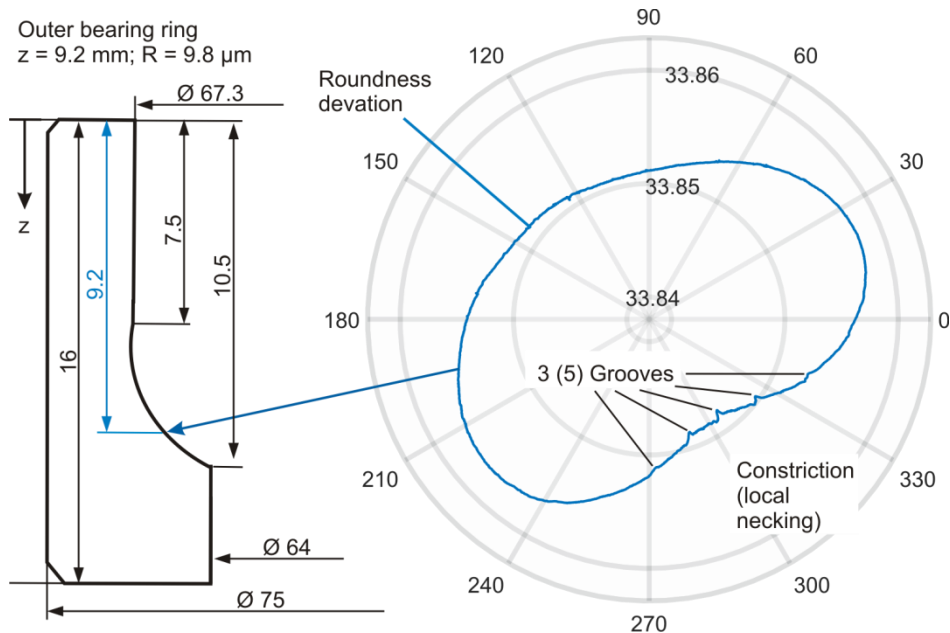


Fig. 3. Deviations from the roundness in the raceway of the outer ring in the front bearing

Analysing the surface of the inner ring reveals considerably more complex damages. Figure 4 shows the geometric roundness test of the inner ring in various z-positions. To measure the bearing ring, it was mounted onto the roundness measuring instrument with the wide side downwards, like the outer ring. On the top right, there is a photo of the measurement with the stylus. On the left-hand side and at the bottom, four roundness measurements in the z-positions of 8.4 mm , 8.8 mm , 9.2 mm and 9.6 mm , each measured from the narrow side, show the plastic deformations.

In the inner ring rotating in the spindle, a smaller roundness deviation can be detected than in the outer ring. The maximum deviation in the inner ring is about $8 \mu\text{m}$.

Regarding the plane at a z-height of 8.4 mm , altogether six about 0.3 to $0.4 \mu\text{m}$ deep grooves at a ball distance of about 17.1° can be seen still a little bit unclear on the right-hand side in the area of polar coordinate angle between 314.4° and 41.5° . Already at this plane, further grooves can be detected at polar coordinate angles between about 128° and 210° . These grooves can be hardly classified owing to an out-of-roundness of max $4.8 \mu\text{m}$. Using an appropriate enlargement, it is, however, possible to detect a certain regularity with regard to the ball distance.

Regarding the plane at a z-height of 8.8 mm , six grooves with a measured depth between 1.4 and $1.9 \mu\text{m}$ are clearly visible in the surface diagram. The grooves are about 2° further turned clockwise, which indicates an inclined groove course. The other grooves can also be clearly seen between angles about 90° and 210° with a depth of about $1 \mu\text{m}$.

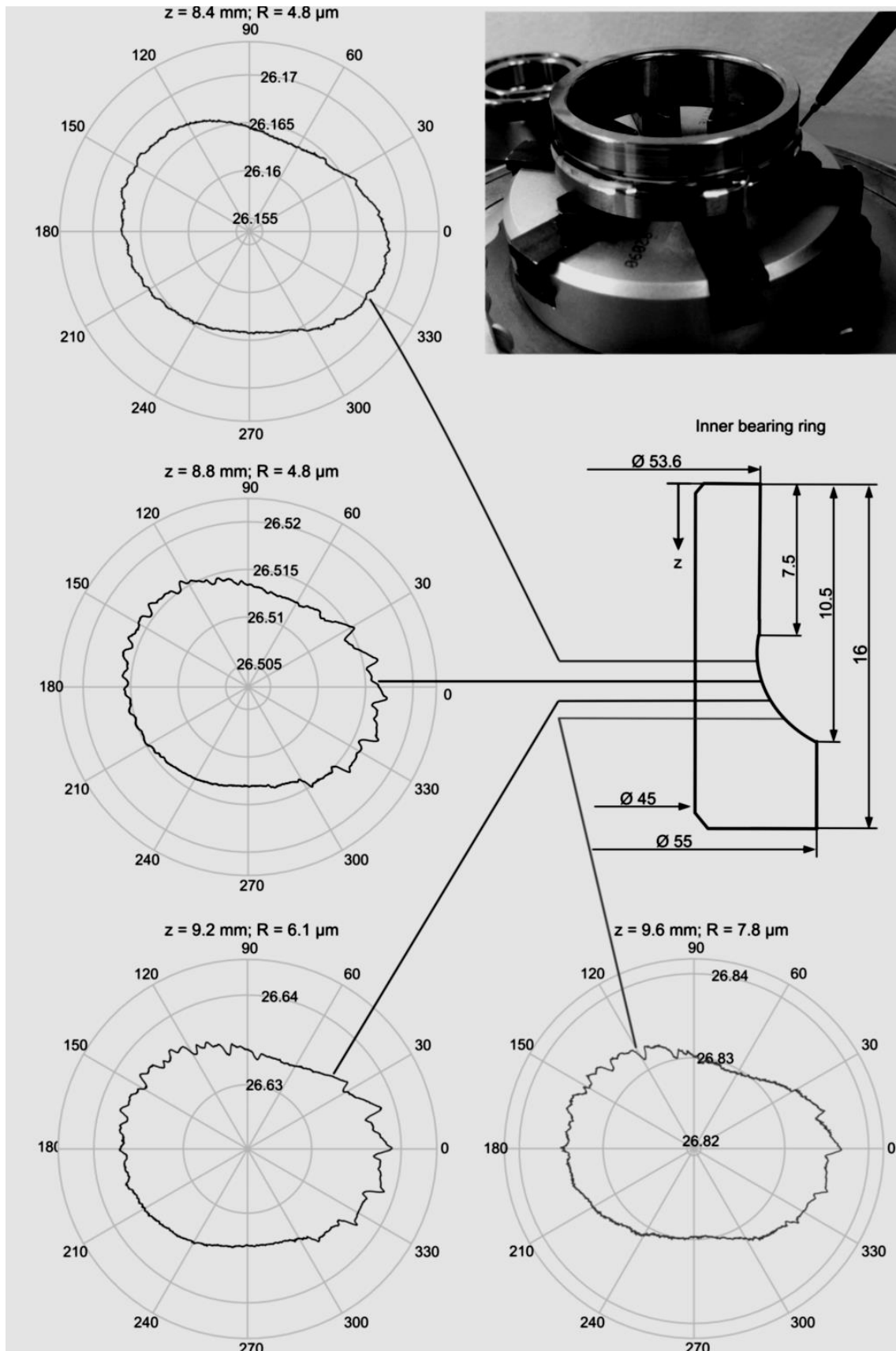


Fig. 4. Deviations from the roundness in the raceway of the inner ring in the front bearing

Regarding a z-height of 9.2 mm, six distinct grooves with 1.0 μm up to 2.2 μm can be detected again. The grooves are now turned clockwise by about another 5°. Behind the groove, an elevation can be clearly seen, which might be explained by the displaced surplus material. In addition, grooves can be seen, for example, at polar coordinate angles of 83.9°, 101.0°, 118.3° etc. The roundness deviation in this plane is 6.1 μm .

Regarding the plane at a z-height of 9.6 mm, only four grooves are clearly visible. The groove depths are considerably lower than at 9.2 mm, even though the deepest groove, measured from the highest elevation to the bottom, is still about 1.9 μm .

4. INFLUENCE OF COLLISIONS ON THE QUIET RUNNING OF BEARINGS

In order to analyse how collisions influence the quiet running of the spindle bearings, the vibrations of the spindle bearings or rather the transmission of the vibrations to the housing is measured. For this purpose, a 3-axis accelerometer was mounted onto the front and the rear bearing seat of the motor spindle. To be able to assess the influence of collisions, run-up analyses are performed to measure the bearing vibrations before and after a collision. As the ball pass frequencies of bearing damages are in proportion to the spindle speed, order analyses are carried out. This allows to directly conclude from the vibrations to the causal mechanism. Figure 5 depicts the test set-up for the order analysis of the spindle.

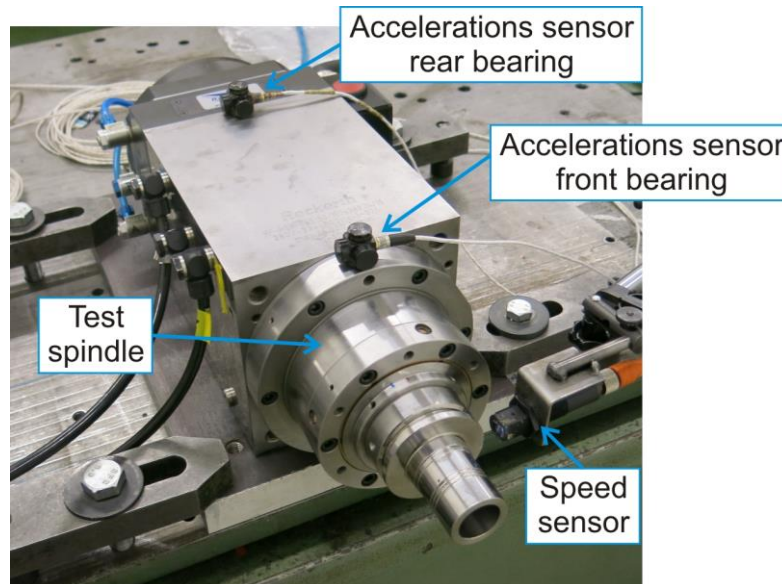


Fig. 5. Test set-up for measuring the quiet running of spindle bearings

Using Equations (1) to (2) for an assumed pitch circle diameter of $D_p = 60.2$ mm, it is now possible to establish the theoretical ball pass frequencies of damages to the rolling bearings. To determine the influence of bearing damages in order analyses, the order is put into the equations instead of the rotational frequency. In this way, it is possible to also take higher-frequency vibration phenomena into account for the respective ball pass frequencies.

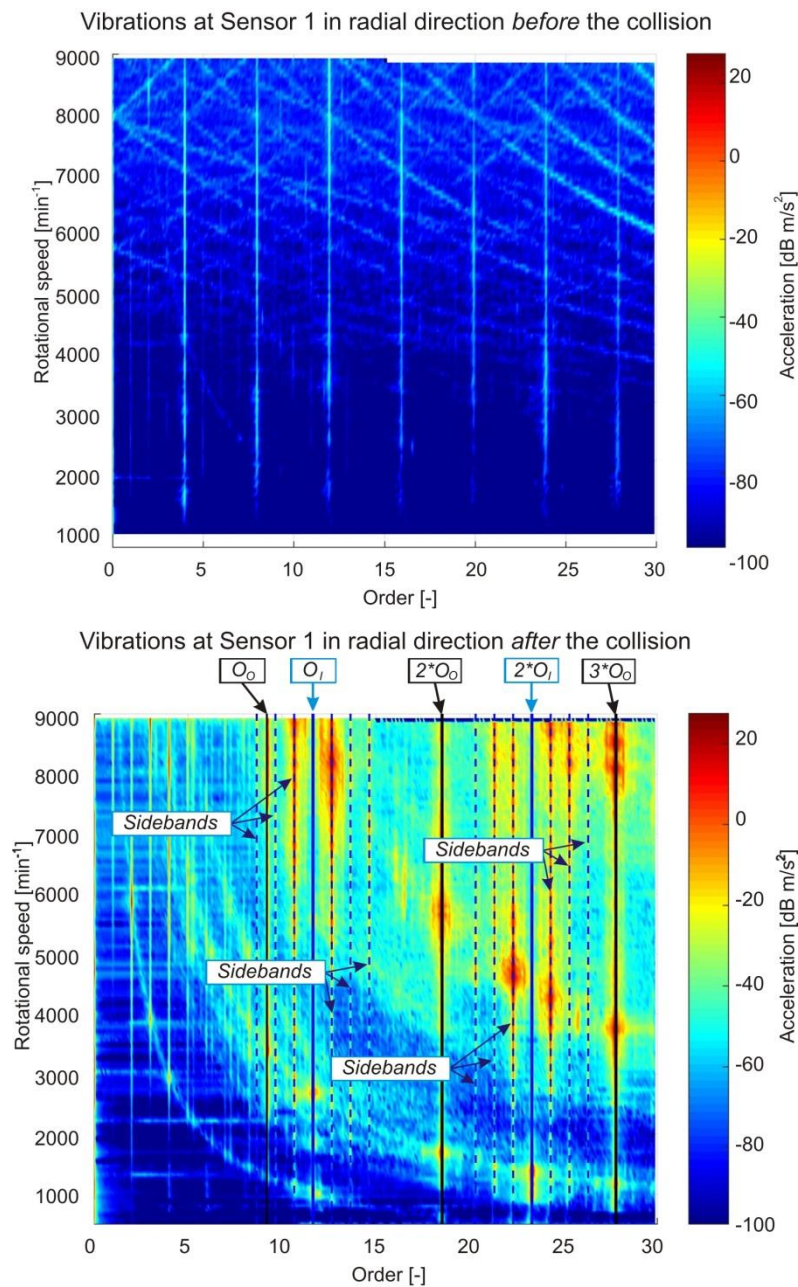


Fig.6. Measuring the quiet running of the bearings (order analysis) [1]

Figure 6 illustrates the spectra of acceleration measured on the bearing seats of the spindle's front main bearing before (top) as well as after the collision (bottom) for a run-up between $n = 1,000 \text{ min}^{-1}$ and $9,000 \text{ min}^{-1}$ up to an order of $O = 30$. In both cases, the measurements were performed at no-load of the spindle. A preload of the tandem-O-arrangement of $F_{pre} = 633 \text{ N}$ here acts as relevant load on the spindle bearings. Thus, the balls of the bearings run through a load zone that is constant depending on the circumference of the bearing, so that indistinct sidebands can be expected. A clear increase in the vibrations arising on the spindle can be detected here. It can be definitely seen that a vibration excitation of the spindle occurs in defined order bands. The electric

motor used can be detected as the only relevant excitation before the collision. It can be recognised via its number of pole pairs ($O_p = 4$) and its multiples in the signals.

Figure 6 at the bottom shows the excited orders and their multiples for the kinematic ball pass frequencies according to Equations (1) and (2) for defects in the inner and outer rings. The arising orders which can be established from this are $O_A = 9.3$ for a defect on the outer ring and $O_I = 11.7$ for a defect on the inner ring. Deviating by less than 1 %, these correspond with the excited order bands measured in the run-up analyses.

In addition, further order bands occur, each at a distance of \pm one, two or three orders from the excited order of a defect in the inner ring. It can be assumed here that these are sidebands of the vibration which are caused by the transverse grooves in the inner bearing ring. Sidebands at a distance of one or two orders from the ball pass frequencies can be explained by the fact that a vertical vibration excitation occurs twice per revolution. The considerably less distinct sidebands at a distance of three or more orders can be attributed to form defects of the bearing rings. In addition, distinct sidebands can be detected for the ball pass frequencies when rolling across a defect in the inner ring.

5. CONCLUSION

A test set-up for simulating collisions was built to analyse how spindle collisions influence the damages to the spindle bearing. In the experiment presented here, a collision between a rotating spindle and an axis was modelled for a kinetic energy of 328 J and a speed of 2.7 m/s. By measuring the roundness of the raceway surface in the inner and outer bearing rings of the spindle in several planes, it was possible to prove the characteristic impressions of the rolling bearings in the form of transverse grooves in the raceway. These occur in the bearings main direction of stress and lead to heavy vibrations of the spindle. By comparing the quiet running of the spindle before and after the collision in the order spectrum, it was possible to establish the characteristic excitation frequencies of the spindle within a frequency range of up to 4500 Hz. The orders excited by the collision could be clearly assigned here to the ball pass phenomena in the inner and outer rings. Hence, the order analysis can be used to draw conclusions about a present spindle collision.

ACKNOWLEDGMENTS

The authors would like to thank Reckerth GmbH for providing the test spindle and actively assisting in the analysis of the experiments.

REFERENCES

- [1] DENKENA B., BERGER J., BLÜMEL P., 2003, *Instandhaltung mit nichtlinearer Dynamik. Eine Methode zur Störungsvorhersage und Prozessoptimierung / Maintenance with nonlinear dynamics. A method for the disturbance forecast and process optimization*, wt Werkstattstechnik online.

-
- [2] HEINZ-SCHWARZMAIER T., 2003, *Bestimmung der Lebensdauer feststoffgeschmierter Kugellager auf der Grundlage von Reibenergieberechnungen und Kurzzeitversuchen*. Dissertation TU Darmstadt. VDI, Düsseldorf.
 - [3] HOEPRICH M.R., 1992, *Rolling element bearing fatigue damage propagation*, Journal of Tribology, 114/2, 328-333.
 - [4] HOSHI T., 2006, *Damage monitoring of ball bearing*, CIRP Annals-Manufacturing Technology, 55, 1427-1430.
 - [5] JACOB E., MANNER P., 2009, *Motorspindelreparatur ist preiswert, erhöht aber die Stillstandszeit*, Maschinenmarkt, Ausgabe, 6, 36-40.
 - [6] KORFF D., 2016, *Schutzmechanismen für Motorspindeln - Ein Beitrag zur Vermeidung kollisionsbedingter Schäden an Werkzeugmaschinen*, Dissertation PTW Darmsatadt, Shaker-Verlag.
 - [7] LACEY S.J., 2015, *Vibration monitoring of rolling bearings to maximise asset reliability*, Schaeffler (UK) Ltd.
 - [8] METZELE M., 2007, *Zustandsorientierte Instandhaltung von schnelllaufenden Werkzeugmaschinen-Hauptspindeln*, Dissertation WZL Aachen, Shaker-Verlag.
 - [9] SCHWÖRER T., BRAUN H.D., 1999, *Milling spindle with collision protection*, European Patent Office, Patenterteilung.
 - [10] WIRTH R., 1998, *Maschinendiagnose an Industriegetrieben-praktische Signalidentifikation*, Antriebstechnik 37, 77-81.